J|A|C|S
ARTICLES
Published on Web 09/15/2006

Observation of Highly Flexible Residues in Amyloid Fibrils of the HET-s Prion

Ansgar B. Siemer,[†] Alexandre A. Arnold,[†] Christiane Ritter,[‡] Thomas Westfeld,[†] Matthias Ernst,[†] Roland Riek,[‡] and Beat H. Meier*,[†]

Contribution from Physical Chemistry, ETH Zurich, CH-8093 Zurich, Switzerland, and Structural Biology Laboratory, The Salk Institute, La Jolla, California 92037

Received May 24, 2006; E-mail: beme@nmr.phys.chem.ethz.ch

Abstract: We report the observation of undetected (until now) residues of the prion protein fragment HET-s(218-289) which give rise to well-resolved ^{13}C, ^{15}N, and ^{1}H NMR resonances under high-resolution magic-angle spinning (HRMAS) conditions. The observed signals belong to large polymeric units as shown by measuring the lateral diffusion constants. The amino acids identified in the spectra are compatible with their localization in the segments of the protein which could not be detected in earlier solid-state NMR experiments. The observed chemical shifts indicate that these residues are in a random-coil conformation. Complementary experiments which detect only dynamic or static residues, respectively, strongly suggest that they belong to different parts of the same molecule.

Introduction

Prion proteins are associated with neurodegenerative diseases in mammals but can also be found in fungi and yeasts.[1,2] The HET-s prion protein of the filamentous fungus *Podospora anserina* is a key player in a genetically controlled cell-death phenomenon called heterocaryon incompatibility. The prion properties of HET-s, including the formation of amyloid fibrils, are essential in this context.[3−6] The protease-resistant part of the prion fibril[7] is formed by the C-terminal domain of HET-s, comprising residues 218-289 (HET-s(218-289)). This fragment alone forms amyloid fibrils and is sufficient for prion propagation.[8] The secondary structure of the fibrils formed in vitro from HET-s(218-289) has recently been characterized using solid-state NMR, H/D exchange data, fluorescence studies, and mutagenesis experiments.[9,10] These studies suggest a structural model containing four well-ordered and rigid β-strands arranged perpendicular to the fibril axis.[9] The core of the fibrils of HET-s(218-289) formed by the β-strands was found to be well ordered and lead to narrow resonance lines but the NMR signals from 29 residues were absent from the spectra. This finding was explained by conformational and/or dynamic disorder of the loops connecting the β-strands and forming the N- and C-terminal ends.[11] The hypothesis of dynamic disorder is supported by the observation that the amide hydrogens of these 29 residues undergo fast hydrogen exchange.[9] Flexible residues are likely to be present in other amyloids, and experimental evidence from NMR is already available, for example in α-synuclein[12] or tau-protein helical fragments.[13] In this work, we report the observation of these so-far undetected residues using liquid-state NMR techniques under HRMAS conditions.[14] Our results show that short segments of HET-s(218-289), even in the close vicinity of well-ordered static residues, can be dynamic enough to average out all anisotropic spin interactions. Consequently, these segments lead to ^{13}C, ^{15}N, and ^{1}H spectra reminiscent of liquid-state NMR when HRMAS[14] is used to remove susceptibility broadening.

Experimental Section

Uniformly ^{13}C,^{15}N-labeled HET-s(218-289) was prepared as described elsewhere.[8,9] Spectra were recorded on a Bruker AV600 spectrometer operating at a static magnetic field of 14.09 T. Spectra with direct ^{1}H detection were recorded on a Bruker 4-mm HRMAS probe spinning at 5 kHz MAS; all other spectra were recorded on a 2.5-mm Varian T3 probe.

For proton-detected spectra, WATERGATE was used for solvent suppression.[15,16] The $^{15}N-^{1}H$ HSQCs were recorded as described by

[†] ETH Zurich.
[‡] The Salk Institute.

(1) Shorter, J.; Lindquist, S. *Nat. Rev. Genet.* **2005**, *6*, 435−450.
(2) Ross, E. D.; Minton, A.; Wickner, R. B. *Nat. Cell Biol.* **2005**, *7*, 1039−1044.
(3) Glass, N. L.; Jacobson, D.; Shiu, P. *Annu. Rev. Genet.* **1997**, *34*, 165−186.
(4) Glass, N. L.; Kaneka, I. *Eukaryotic Cell* **2003**, *2*, 1−8.
(5) Saupe, S. J. *Microbiol. Mol. Biol. Rev.* **2000**, *64*, 489−502.
(6) Saupe, S. J.; Clave, C.; Begueret, J. *Curr. Opin. Microbiol.* **2000**, *3*, 608−612.
(7) Maddelein, M. L.; Dos Reis, S.; Duvezin-Caubet, S.; Coulary-Salin, B.; Saupe, S. J. *Proc. Natl. Acad. Sci. U.S.A.* **2002**, *99*, 7402−7407.
(8) Balguerie, A.; Dos Reis, S.; Ritter, C.; Chaignepain, S.; Coulary-Salin, B.; Forge, V.; Bathany, K.; Lascu, I.; Schmitter, J.-M.; Riek, R.; Saupe, S. J. *EMBO J.* **2003**, *22*, 2071−2081.
(9) Ritter, C.; Maddelein, M. L.; Siemer, A. B.; Luhrs, T.; Ernst, M.; Meier, B. H.; Saupe, S. J.; Riek, R. *Nature* **2005**, *435*, 844−848.
(10) Siemer, A. B.; Ritter, C.; Steinmetz, M. O.; Ernst, M.; Riek, R.; Meier, B. H. *J. Biomol. NMR* **2006**, *34*, 75−87.
(11) Siemer, A. B.; Ritter, C.; Ernst, M.; Riek, R.; Meier, B. H. *Angew. Chem., Int. Ed.* **2005**, *44*, 2441−2444.
(12) Heise, H.; Hoyer, W.; Becker, S.; Andronesi, O. C.; Riedel, D.; Baldus, M. *Proc. Natl. Acad. Sci. U.S.A.* **2005**, *102*, 15871−15876.
(13) Sillen, A.; Wieruszeski, J. M.; Leroy, A.; Ben Younes, A.; Landrieu, I.; Lippens, G. *J. Am. Chem. Soc.* **2005**, *127*, 10138−10139.
(14) Elbayed, K.; Dillmann, B.; Raya, J.; Piotto, M.; Engelke, F. *J. Magn. Reson.* **2005**, *174*, 2−26.
(15) Piotto, M.; Saudek, V.; Sklenar, V. *J. Biomol. NMR* **1992**, *2*, 661−665.

10.1021/ja063639x CCC: $33.50

Mori et al.,[17] and $^{13}C-^{1}H$ HMQCs were measured with the scheme of Andersson et al.,[18] both experiments using GARP[19] decoupling with an rf-field strength of 6 kHz for ^{15}N and 4.5 kHz for ^{13}C, during acquisition. For the $^{15}N-^{1}H$ HSQC 192 t_1-experiments with 64 scans each, for the $^{13}C-^{1}H$ HMQC 1536 t_1-experiments with 14 scans each were acquired in a total measurement time of 8.5 h, and 13 h, respectively.

The clean adiabatic TOCSY experiments followed the experimental scheme of Kupce et al.[20,21] using 200 μs WURST-2 pulses[22] and an overall mixing time of 50 ms. GARP decoupling on ^{15}N and ^{13}C was applied during t_1 and t_2.

Three experiments with TOBSY transfer and a different preparation step were performed. The adiabatic TOBSY experiment was done as described by Hardy et al.[23] The WiW^{1}_{24} sequence at 24.242 kHz MAS with WURST-5 pulses was used for mixing. The length of the WURST pulses was 55 μs, and the mixing time was 7.9 ms. XiX ^{1}H decoupling[24] was applied during t_1 and t_2, and LG decoupling[25] was applied during mixing, both with an rf-field strength of 150 kHz. The initial polarization of these spectra was either generated by cross polarization, by NOE presaturation followed by direct excitation, or by a refocused INEPT transfer. The measurement times for the three experiments were 27, 27, and 54 h, respectively. All 2D-spectra were analyzed using the CARA program.[26]

Diffusion coefficients were measured using the LED pulse sequence with bipolar gradients.[27] The total gradient pulse length was $\delta = 4$ ms, the diffusion time $\Delta = 50$ ms, and the eddy current delay $T_e = 5$ ms. Sine-shaped gradients were used, and their strength was incremented in 32 steps between $g = 3.9 \times 10^{-2}$ T/m and 35.7×10^{-2} T/m. The diffusion coefficients were calculated by assuming a single diffusion coefficient and fitting the intensity decay curves with the equation $I(q) = I(q) \exp[-Dq^2(\Delta - \delta/3 - \tau/2)]$ with $q = \gamma\delta g$ where γ is the gyromagnetic ratio and $\tau = 200$ μs is the delay for gradient switching.

Results and Discussion

One-dimensional ^{1}H spectra of the amyloid fibrils of uniformly ^{15}N,^{13}C-labeled HET-s(219-289) are shown in Figure 1a. Without MAS ("static"), no protein signals can be resolved, and the spectrum is dominated by the water resonance, massively broadened by magnetic susceptibility effects. HRMAS at a spinning frequency as slow as $\nu_r = 500$ Hz was sufficient to obtain narrow ^{1}H lines. Water presaturation reduces considerably the intensity of the whole spectrum as can be seen in Figure 1a, second trace. The ^{1}H line width observed with $\nu_r = 5$ kHz was, for the aliphatic resonances, in the range of 0.03−0.08 ppm (20−50 Hz).

To demonstrate that these sharp resonances indeed come from fibrils and not from free monomers or small aggregates, a ^{1}H NMR spectrum of the supernatant, obtained after mild centrifugation (10 min at 3500*g*), was recorded. This spectrum did not contain any protein-typical resonances (data not shown), excluding the possibility that the signals come from dissolved HET-s(218-289) monomers. To further characterize the size of the observed entities, pulsed-field gradient methods were used to estimate the molecular diffusion constant[28] (see Experimental Section for details). The measured diffusion constant of the protein is 42 times slower than the one for the shift-reference DSS used as an internal standard.[29] Using the Stokes−Einstein relation, the size of the particle can, therefore, be estimated to be in the order of 16 MDa. This result excludes the possibility that the narrow lines are caused by dissolved HET-s(218-289) molecules or small aggregates thereof.

The narrow linewidths in the spectra allowed us to record two-dimensional spectra using liquid-state pulse sequences under

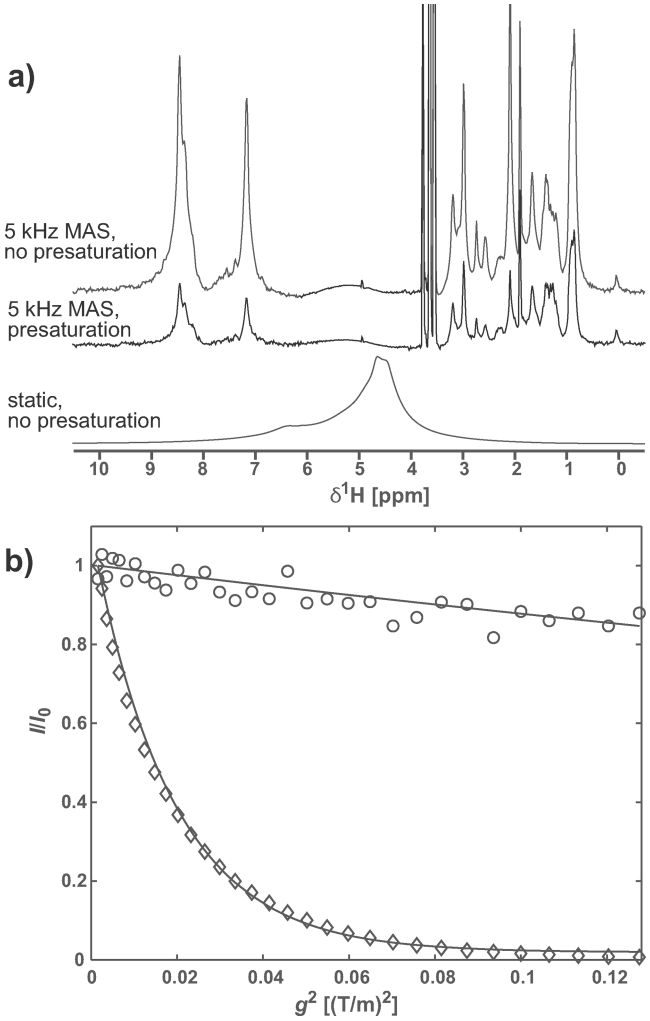

Figure 1. (a) One-dimensional ^{1}H NMR spectra of amyloid fibrils of ^{15}N,^{13}C-labeled HET-s(218-289) recorded using a Bruker 4 mm HRMAS probe. For the static spectrum no water suppression was applied, and 256 scans were recorded. For the spectra at 5 kHz MAS WATERGATE water suppression was applied, and 768 scans were recorded. The water-selective presaturation was done with an rf-field strength of 150 Hz. (b) Experimental diffusion decay curves under the LED pulse sequence with bipolar gradients. The data shown are representative of the decay of the sharp lines belonging to the protein (circles). DSS which was used as an internal molecular weight reference ($M = 218$ Da) is shown in diamonds. The best fits assuming a single diffusion constant are also plotted. The corresponding diffusion coefficients are $D = 5.0 \times 10^{-11}$ m^2 s^{-1} (protein) and $D = 2.1 \times 10^{-9}$ m^2 s^{-1} (DSS).

(16) Liu, M. L.; Mao, X. A.; Ye, C. H.; Huang, H.; Nicholson, J. K.; Lindon, J. C. *J. Magn. Reson.* **1998**, *132*, 125−129.
(17) Mori, S.; Abeygunawardana, C.; Johnson, M. O.; Vanzijl, P. C. M. *J. Magn. Reson., Ser. B* **1995**, *108*, 94−98.
(18) Andersson, P.; Gsell, B.; Wipf, B.; Senn, H.; Otting, G. *J. Biomol. NMR* **1998**, *11*, 279−288.
(19) Shaka, A. J.; Barker, P. B.; Freeman, R. *J. Magn. Reson.* **1985**, *64*, 547−552.
(20) Kupce, E.; Schmidt, P.; Rance, M.; Wagner, G. *J. Magn. Reson.* **1998**, 135, 361−367.
(21) Kupce, E.; Hiller, W. *Magn. Reson. Chem.* **2001**, *39*, 231−235.
(22) Kupce, E.; Freeman, R. *J. Magn. Reson., Ser. A* **1995**, *117*, 246−256.
(23) Hardy, E. H.; Detken, A.; Meier, B. H. *J. Magn. Reson.* **2003**, *165*, 208−218.
(24) Detken, A.; Hardy, E. H.; Ernst, M.; Meier, B. H. *Chem. Phys. Lett.* **2002**, *356*, 298−304.
(25) Lee, M.; Goldburg, W. I. *Phys.Rev.* **1965**, *140*, A1261−A1271.
(26) Keller, R. L. J. *The Computer Aided Resonance Assignment Tutorial*; Cantina Verlag: Goldau, 2004. (See also http:/ www.nmr.ch.)
(27) Wu, D. H.; Chen, A. D.; Johnson, C. S. *J. Magn. Reson., Ser. A* **1995**, *115*, 260−264.
(28) Stejskal, E. O.; Tanner, J. E. *J. Chem. Phys.* **1965**, *42*, 288−292.
(29) Jones, J. A.; Wilkins, D. K.; Smith, L. J.; Dobson, C. M. *J. Biomol. NMR* **1997**, *10*, 199−203.

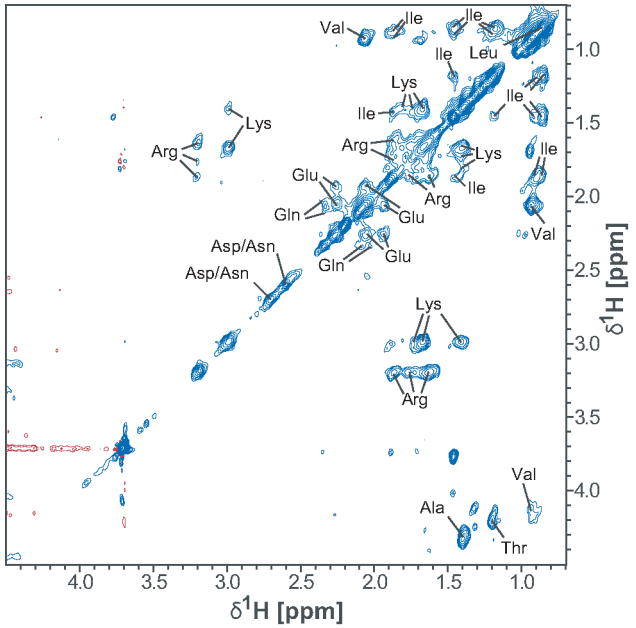

Figure 2. Two-dimensional $^{1}H-^{1}H$ TOCSY spectrum of amyloid fibrils of $^{15}N,^{13}C$-labeled HET-s(218-289) recorded at 5 kHz MAS in a 4-mm HRMAS probe at 30 °C. The mixing time was 50 ms. Contour levels start at 2.5 times rms-noise level and increase by a factor of 1.4.

HRMAS. The $^{1}H-^{1}H$ TOCSY spectrum[20,30] of amyloid fibrils is shown in Figure 2, the $^{1}H-^{13}C$ HMQC and the $^{1}H-^{15}N$ HSQC spectra are given in Figure 3. Thirteen different amino acids could be identified tentatively from these spectra, namely, Ala, Arg, Asn, Asp, Gln, Glu, His, Ile, Leu, Lys, Thr, Val, and Met. The chemical shifts of the corresponding resonances are given in the Supporting Information. We were not able to detect any protein−protein cross peaks in the $^{1}H-^{1}H$ NOESY spectra recorded with mixing times in the range of $\tau_m = 20-750$ ms (data not shown), and no sequential assignment is currently available for the mobile residues.

From the measured shifts of the H^{α}, C^{α}, and C^{β} resonances conclusions about the secondary structure of the protein can be drawn. All shifts are consistent with a random-coil arrangement (see Supporting Information). This interpretation is also supported by the narrow overall distribution of the chemical shifts in the $^{1}H-^{15}N$ HSQC spectrum of Figure 3b. These observations are evidence that the residues observed in the spectra come from parts of the protein that have no well-defined secondary structure and are highly dynamic, showing an almost isotropic local mobility. All amino acids detected appear either in the long loop or in the head and tail pieces of the molecular structure model described in ref 9. These molecular segments are marked with black letters in Figure 4d. There is one exception, however, namely the amino acid Glu whose presence could be explained by deamidation of a Gln.[31,32] Note that the purification of HET-s(218-289) included stages at low pH.[8] The amino acid His only appears in the long loop and at the C-terminus; Met appears only at the N-terminus of HET-s(218-289). However, all the other amino acids detected above appear also in the β-strand part of the molecule whose resonances were assigned earlier by solid-state NMR techniques (residues marked in red letters in Figure 4d). Despite the fact that many of the residues in question appear more than once in the black segment, no obvious peak doubling is observed in the spectra, indicating that either only one of these residues is observable or that their chemical shifts are almost degenerate. The latter was also observed for liquid silk proteins inside the gland of a spider.[33]

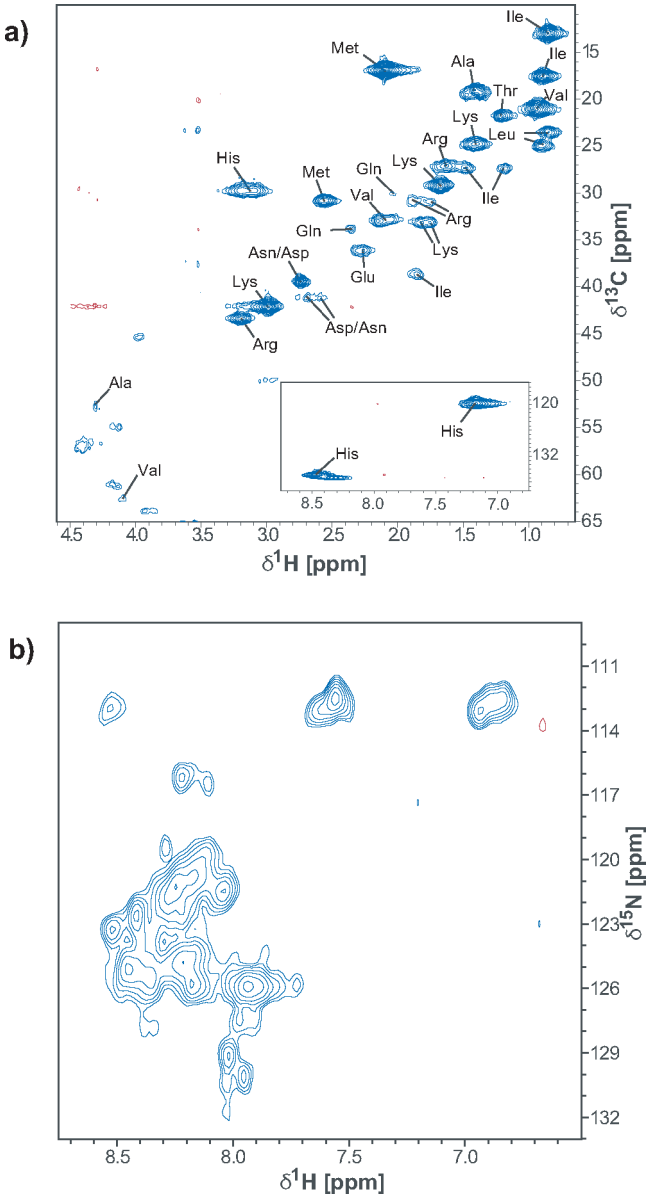

Figure 3. $^{1}H-^{13}C$ and $^{1}H-^{15}N$ correlation spectra of amyloid fibrils of uniformly labeled HET-s(218-289) recorded at 5 kHz MAS in a 4-mm HRMAS probe. (a) $^{1}H-^{13}C$ HMQC at 5 °C, tentative assignments are indicated. (b) $^{1}H-^{15}N$ HSQC at 30 °C.

To further discriminate between the mobile and rigid parts, we have recorded $^{13}C-^{13}C$ TOBSY spectra that filter out selectively either mobile or immobile parts of the sample, or show all resonances. The TOBSY polarization transfer is mediated by the isotropic J couplings and has the same efficiency for mobile and rigid systems. For liquid samples, the TOBSY sequence has properties equivalent to those of TOCSY. In anisotropic phase, TOBSY additionally suppresses the dipolar interaction as a transfer mechanism.[34,35] The filtering is imple-

(30) Braunschweiler, L.; Ernst, R. R. *J. Magn. Reson.* **1983**, *53*, 512−528.
(31) Wright, H. T. *Crit. Rev. Biochem. Mol. Biol.* **1991**, *26*, 1−52.
(32) Scotchler, J. W.; Robinson, A. B. *Anal. Biochem.* **1974**, *59*, 319−322.
(33) Hronska, M.; van Beek, J. D.; Williamson, P. T. F.; Vollrath, F.; Meier, B. H. *Biomacromolecules* **2004**, *5*, 834−839.
(34) Baldus, M.; Meier, B. H. *J. Magn. Reson., Ser. A* **1996**, *121*, 65−69.

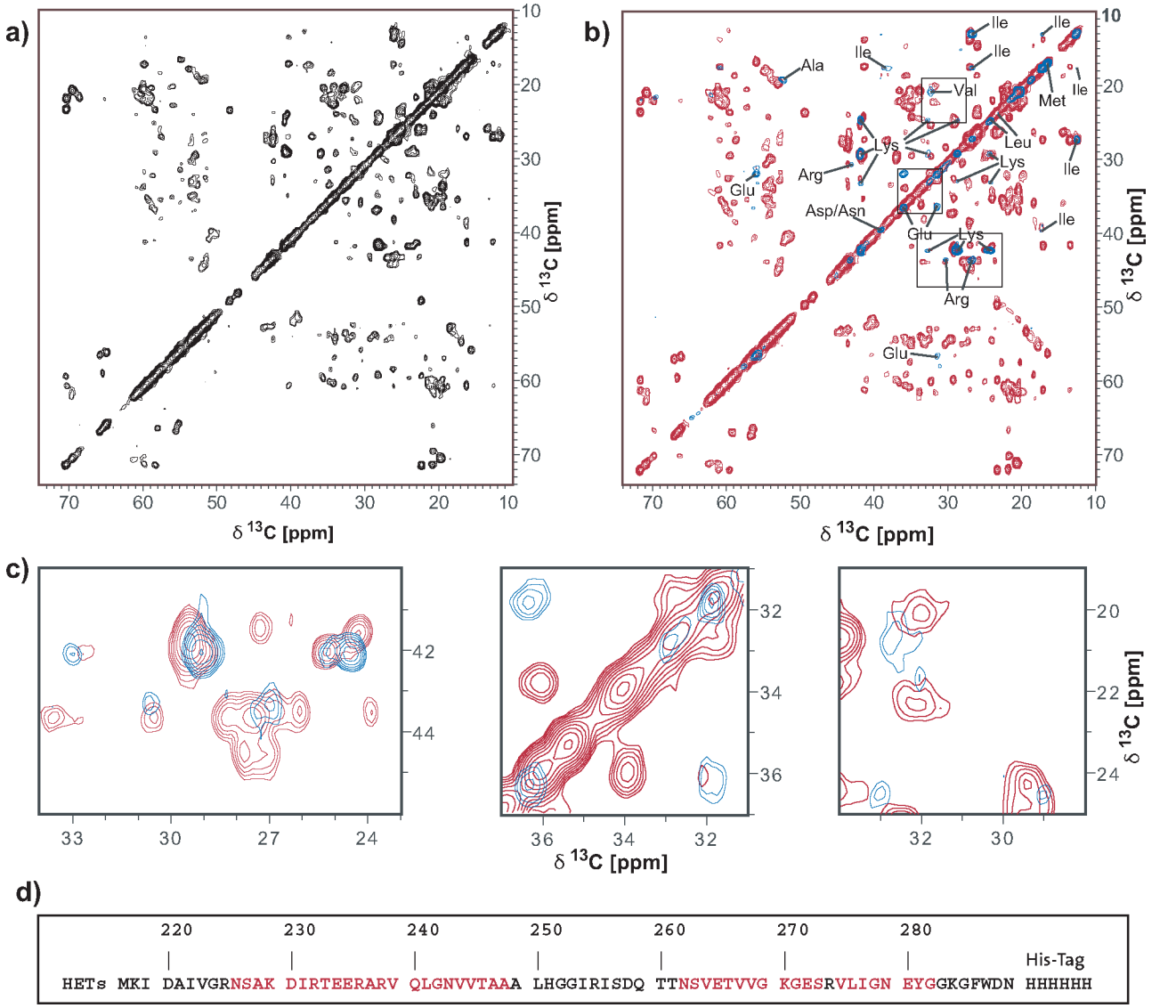

Figure 4. (a,b) $^{13}C-^{13}C$ adiabatic TOBSY spectra of amyloid fibrils of $^{15}N,^{13}C$-labeled HET-s(218-289) recorded in a 2.5-mm solid-state MAS probe at 24.242 kHz MAS and 7.9 ms mixing time. The spectra based on initial magnetization coming from NOE-enhancement and direct excitation (a), CP (b), and refocused INEPT (b) are colored in black, red, and blue, respectively. (c) Enlargements of the regions indicated in (b). (d) Amino acid sequence of HET-s(218-289) with residues assigned using dipolar-based solid-state NMR methods[10] colored in red.

mented in the preparation step for the ^{13}C magnetization prior to the t_1 period of the experiment: when (i) polarization is transferred from the protons using an INEPT step, immobile parts are filtered out because sizeable proton−proton dipolar interactions lead to a fast decay of the transverse magnetization in the free evolution periods of the INEPT preparation. The resonances from the static part are then missing in the TOBSY spectrum. In contrast, when (ii) a cross-polarization step is used for the polarization transfer, mobile segments are filtered out because (heteronuclear) dipolar interactions are required for efficient cross polarization. As a further option, (iii) ^{13}C magnetization can be prepared by a single ^{13}C 90° pulse, with NOE presaturation, which leads to signals from the mobile as well as immobile parts. The corresponding spectra are shown in Figure 4. Filtering for mobile components leads to the blue spectrum of Figure 4b, and filtering for immobile parts leads to the red spectrum. Nonselective excitation yields the TOBSY spectrum in Figure 4a which qualitatively can be interpreted as the sum of the two spectra in 4b. The red TOBSY spectrum of the immobile parts of HET-s(218-289) is very similar to a dipolar DREAM spectra of HET-s(218-289) fibrils.[9] As emphasized in Figure 4c the blue resonances of the mobile part represent largely *additional* resonances. The fact that all the previously assigned peaks are also found in Figure 4a and that the resonance intensities for the blue and red resonances are similar supports the interpretation that the molecular segments that give rise to the blue peaks and the sharp proton lines in Figures 1−3 indeed come from the same molecules as do the red peaks and that they represent the mobile loops of the molecular structure. The interpretation that they come from a second conformer of the HET-s(218-289) molecule seems, in the light of these data, unlikely but can not rigorously be excluded. It is interesting to remark that no Leu or Gln residues can be found in the head and tail segments of the molecules, their presence on the liquid-type spectra would thus indicate that the 13-amino-acid loop between β-strands 2 and 3 also contributes to the mobile fraction.

(35) Baldus, M.; Iuliucci, R. J.; Meier, B. H. *J. Am. Chem. Soc.* **1997**, *119*, 1121−1124.

We note that the unfiltered spectrum of Figure 4a or, equivalently, the sum of the two spectra in Figure 4b still does not contain the resonances from all amino-acid residues. At least eight residues are missing (5 Gly, Ser, Phe, Trp). It is our conjecture that these residues are structurally disordered and less mobile or/and undergo a slow conformational exchange, leading to broad lines in all spectra. It should also be noted that the observed resonances are mainly assigned to side-chain atoms which explains the missing Gly resonances.

Conclusion

In summary, we have reported the existence of highly flexible amino-acid residues in a sample of HET-s prion protein fragment 218-289 in its amyloid state. The mobility leads to sharp proton resonance spectra under HRMAS conditions, indicating that the averaging by the local motion is almost complete. The resonances representing highly dynamic residues come from large particles, and there is strong evidence that they belong to the segments framing the β-sheets in the structural model of ref 9. This study thus refines the model of the HET-s prion protein and emphasizes the possibility of significant dynamic heterogeneity in amyloids. It can be hypothesized that this high flexibility enables optimal β-sheet formation, thus explaining the high degree of order in it.[11] The highly mobile regions are water accessible. The study of these highly mobile and accessible parts could be of importance for understanding prion interaction with drugs or membranes.

Acknowledgment. Financial support by the Swiss National Science Foundation is acknowledged.

Supporting Information Available: Table of chemical shifts of assigned amino acids, comparison of the measured chemical shifts with respective random-coil, β-strand, and α-helical values. This material is available free of charge via the Internet at http://pubs.acs.org.

JA063639X